Journal of Thermal Science Vol.30, No.1 (2021) 210–219

https://doi.org/10.1007/s11630-020-1288-0 **Article ID: 1003-2169(2021)01-0210-10**

Numerical Simulation Study on Cooling Characteristics of a New Type of Film Hole

GUO Chunhai[1*], WANG Bin[1], KANG Zhenya[2], ZHANG Wenwu[1], ZHENG Huilong[2]

1. Ningbo Institute of Materials Technology and Engineering, Chinese Academy of Sciences, Ningbo 315201, China
2. Institute of Engineering Thermophysics, Chinese Academy of Sciences, Beijing 100190, China

Abstract: A new type of film cooling hole with micro groove structure is presented in this paper. Based on the finite volume method and the Realizable k-ε model, the film cooling process of the hole in a flat plate structure is simulated. The surface temperature distribution and film cooling effect of different film cooling holes were analyzed. The effects of micro-groove structure on wall attachment and cooling efficiency of jet were discussed. The results show that under the same conditions, the transverse coverage width and overall protective area of the new micro-groove holes are larger than those of the ordinary cylindrical holes and special-shaped holes. Compared with ordinary holes, the new micro-groove holes can better form the film covering on the surface and enhance the overall film cooling efficiency of the wall. For example, when the blowing ratio M=1.5, the effective coverage ratio of micro-groove holes is 1.5 times the dustpan holes and is 8 times the traditional cylindrical holes. It provides reference data and experience rules for the optimization and selection of advanced cooling structure of high performance aero-gas engine hot-end components.

Keywords: film cooling, shaped hole, numerical simulation, optimal design, cooling efficiency

1. Introduction

The thrust and thermal efficiency of the aero gas turbine engine increase with the increase of the inlet temperature of turbine. In order to ensure the safe and reliable operation of turbine blades in high temperature gas environment, cooling and thermal protection measures must be taken for the blades. Film cooling is a widely used effective cooling protection technology. Accurate prediction of film cooling effect plays an important role in turbine blade design. Film cooling is the interaction between internal cooling gas jet and high temperature gas, forming a cooling protective film between the external wall and high temperature gas. In the high temperature gas path, the discrete film cooling geometry structure forms a continuous film protective layer on the whole surface by applying efficient film cooling technology. It can build a good defense line under the violent impact of high heat flux gas, and directly reduce the heat flux of convection into the wall. In the first decades, film cooling technology was limited to simple circular holes perpendicular to or at a certain angle to the surface. Later, special-shaped holes and combined cooling units were developed to achieve higher adiabatic film cooling efficiency than circular film cooling holes.

In the early 1970s, Goldstein et al. [1, 2] made a very good overview of the early research on film cooling

Received: May 20, 2019 Corresponding author: GUO Chunhai E-mail: guochunhai@nimte.ac.cn

Nomenclature

A_f	effective film coverage ratio	T_c	temperature of jet flow/K
a_f	effective gas film coverage area/m^2	T_∞	temperature of mainstream/K
a_h	cross section area of channel/m^2	t	time/s
C_p	heat capacity at constant pressure/$J\cdot kg^{-1}\cdot K^{-1}$	U_c	velocity of jet flow/$m\cdot s^{-1}$
D	inlet diameter of the jet hole/m	U_∞	velocity of mainstream/$m\cdot s^{-1}$
H_d	height of main channel/m	V	velocity vector field/$m\cdot s^{-1}$
I	unit tensor	$\vec{v}$	velocity vectors in the x, y, z/$m\cdot s^{-1}$
k	heat conduction coefficient/$W\cdot m^{-1}\cdot K^{-1}$	W_d	width of main channel/m
L	length of jet channel/m	W_1	width of part of micro-groove/m
L_1	length of the cylindrical part of jet channel/m	**Greek symbols**	
L_d	length of main channel/m	α	injection angle/°
M	blowing ratio $M = \rho_c U_c / \rho_\infty U_\infty$	δ	lateral expansion angle/°
P_c	pressure of jet flow/Pa	η	film-cooling effectiveness
P_∞	pressure of mainstream/Pa	θ	streamwise expansion angle/°
p	pressure/Pa	μ	viscosity coefficient/$N\cdot s\cdot m^{-2}$
S_T	viscous dissipation term	ρ	density/$kg\cdot m^{-3}$
T	temperature/K	ρ_c	density of jet flow/$kg\cdot m^{-3}$
T_{aw}	temperature of adiabatic wall/K	ρ_∞	density of mainstream/$kg\cdot m^{-3}$

related to basic film geometry. The film cooling performance of the special shaped hole was first demonstrated and its quantitative analysis was carried out. It was found that the special-shaped holes exhibited excellent adhesion of jet to the wall. Kruse et al. [3] found that the circular film cooling hole jet showed a clear horseshoe curl vortex at the upstream interaction point, and then wrapped around the jet. Immediate effects occur after the outlet of the hole, i.e. the so-called swirling pair, where two currents meet and rise to create separation zones. The airflow interaction causes the high temperature gas to move below the cooling jet, resulting in the reduction of cooling efficiency. Haven et al. [4] measured the development of jet flow structure in a special-shaped film cooling hole by planar laser-induced fluorescence. The so-called counter-vorticity pair structure exists in the plane structure downstream of the special-shaped hole, which is contrary to the development of the vortices of the circular hole jet. The results show that a larger inclination of the extended side can make the coolant expand better on the surface and reduce mixing with high temperature air flow. On the basis of it, Bunker [5] studied hypersonic jet. The actual heavy-duty gas turbine blades were used in the jet experiment, and the film holes including coating were processed by standard methods. The film cooling efficiency of the basic data is very important for engine design, especially for the analysis data of main parameters affecting film cooling performance under conditions similar to engine working environment. Lu et al. [6] carried out experimental and numerical studies on the cooling performance of film holes in six different grooves. The results show that the cooling efficiency of cylindrical film holes decreases with the increase of blowing ratio, but the cooling efficiency of grooved film holes does not change significantly. Lee and Kim [7] improved the cooling effect by optimizing the ratio of length to diameter of cylindrical holes and the incidence angle of cooling air. Kim et al. [8] improved cooling efficiency by optimizing the inlet shape of cylindrical holes. The results show that compared with the simple cylindrical hole, the optimized hole improves the film cooling efficiency by 46.5%. Davidson et al. [9] experimentally studied the effect of film cooling geometry on the cooling performance of thermal conductive turbine blades with thermal barrier coatings (TBC). The results show that the coverage area of grooves and improved grooves is larger than that of round holes. However, the temperature improvement at the interface of TBC and blade wall is not obvious. Zhang et al. [10] numerically simulated film cooling of round-to-slot holes on a plane. It is found that the diffusion from circular hole to groove hole has a good effect on the enhancement of film cooling near the film hole. However, at a certain distance, the average film cooling effect of the flow direction of the pore structure is not much different from that of the straight circular hole. Zhang et al. [11] carried out an experimental and numerical study on the heat transfer and flow characteristics of a lateral outlet channel. They found that a long low-speed vortex was

formed in the lateral outlet passage and became smaller with the rotation of the vortex.

So far, there are many institutions and related literatures to study film cooling technology directly or indirectly [12–19]. The main research issues are mainly focused on exploring the hydrodynamics inside the film hole, turbulent flow and vorticity, the entry mode of the air flow at the front end of the hole entrance, the shape, direction and spatial arrangement of the film hole, the length-diameter ratio of the film hole, the density ratio, blowing ratio and momentum ratio of the jet to the mainstream gas, the turbulent intensity of the mainstream, and the acceleration of the mainstream. The influence of degree, external wall curve parameters and external wall roughness on cooling efficiency is one of the factors affecting the design. The possible changing conditions make the design very difficult.

In this paper, a new type of micro-groove film cooling hole is studied to improve the cooling effect of the film. The Navier-Stokes equation was used to analyze the flow and film cooling. Compared with traditional cylindrical holes and special-shaped holes of dustpan, the effect of micro-groove holes on film cooling performance was determined.

2. Physical Model and Computational Conditions

2.1 Geometric model and mesh generation

The geometric structure is shown in Fig. 1. Flat film cooling holes are used as geometric models; the main channel is rectangular, and the jet channel is film cooling holes. The length, width and height of main channel are respectively L_d=60D, W_d=10D, H_d=4D. The distance of film cooling holes outlet from the entrance of mainstream computational domain is 5D. They are cylindrical hole, special-shaped hole of dustpan and special-shaped hole of micro-groove structure respectively. The special-shaped hole of dustpan is deformed on the basis of cylindrical hole. The special-shaped hole of micro-groove structure is composed of part of cylindrical hole and part of micro-groove. The injection angle is α=30°, and the channel of the jet is L/D=8. The flow expansion angle forward of dustpan θ=10°, lateral expansion angle δ=15°, L_1/L=0.4, the width of micro-groove is 5W_1=10D.

The computational model uses unstructured hybrid grids. The main channel adopts hexahedral structure mesh, and the jet channel adopts tetrahedral unstructured mesh. The boundary layer is near the wall, and the mesh is encrypted in the mixed region. The key areas are refined by grid, and the irregularity of the hole is fused by interface to plan the grid distribution of the whole calculation area reasonably. Among them, the number of meshes in the film hole is more than 2×10^5; the total number of meshes is more than 4×10^6, and the y^+ on the exit surface of the film hole is less than 5, which meets the calculation requirements.

The fluid medium in this paper is ideal gas. The main inlet boundary is the normal velocity inlet and the mainstream temperature is given. At the entrance of the cooling air jet-flow, the normal velocity entrance is also given. Its size is determined by the blowing ratio (M = 0.5, 1.0 and 1.5), and the temperature of the cooling air is a fixed value. The boundary condition at the outlet of main channel is pressure outlet, and the relative pressure is 0. Non-slip adiabatic wall boundary conditions are adopted on the walls of holes and channel. Because some film holes are calculated in this paper, periodic boundary conditions are applied on both sides of the main channel. In addition, the turbulence intensity at the mainstream entrance is 3%.

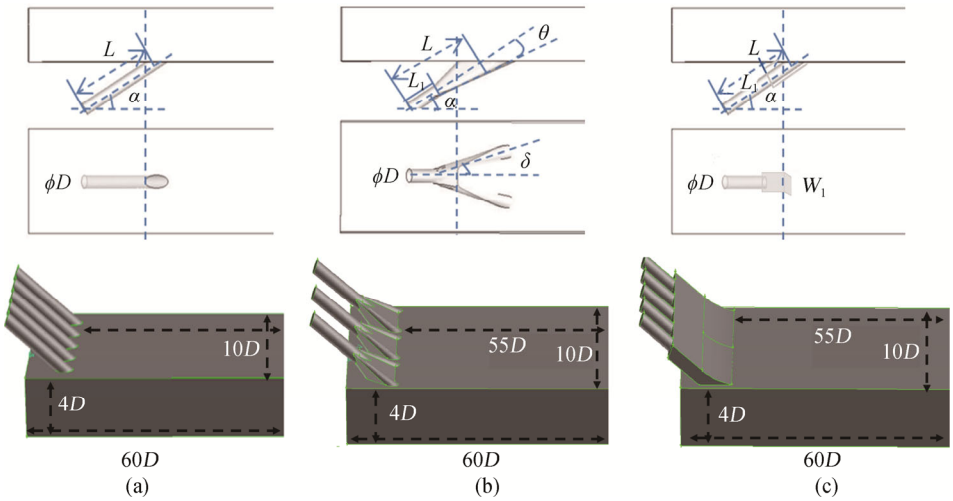

Fig. 1 Geometry of film cooling holes and computational domain: (a) cylindrical hole, (b) special-shaped hole of dustpan and (c) special-shaped hole of micro-groove structure

2.2 The turbulence model for film cooling process

In the process of high-speed film flow, the flow is turbulent. The continuous equation, momentum equation and energy equation in Reynolds average N-S equation are used to describe the flow process. The expressions are as follows:

$$\frac{\partial \rho}{\partial t}+\nabla\cdot\left(\rho\vec{v}\right)=0 \tag{1}$$

$$\frac{\partial\left(\rho\vec{v}\right)}{\partial t}+\nabla\cdot\left(\rho\vec{v}V\right)=-\nabla p+\nabla\cdot\left[\mu\left(\nabla\vec{v}+\nabla\vec{v}^{T}\right)-\frac{2}{3}\mu\nabla\cdot\vec{v}I\right] \tag{2}$$

$$\frac{\partial\left(\rho T\right)}{\partial t}+\nabla\cdot\left(\rho\vec{v}T\right)=\nabla\cdot\left(\frac{k}{c_p}\nabla T\right)+\frac{S_T}{c_p} \tag{3}$$

where t, ρ, p and T represent time, density, static pressure and temperature; $\vec{v}$ represents the velocity vectors in three directions x, y and z respectively. And μ, c_p, k, S_T and I represent viscosity coefficient, heat capacity at constant pressure ratio, heat conduction coefficient, viscous dissipation term and unit tensor. The velocity vector field in Cartesian coordinates is $V=ui+vj+wk$, $\nabla=i\frac{\partial}{\partial x}+j\frac{\partial}{\partial y}+k\frac{\partial}{\partial z}$. The above i, j and k denote x, y, z direction unit vectors, respectively.

The RNG model (renormalization model) is used as the turbulence viscosity model. Compared with other models, the model takes into account the effects of high-speed shear and eddy currents in the basin, and also the viscous effect at low Reynolds number. Combining with the wall function, the model can solve the flow problems in the fully developed turbulent region and the near wall region more accurately and reliably. The transport equation of the RNG model is similar to that of the standard model. Its expression is as follows:

$$\frac{\partial}{\partial t}\left(\rho k\right)+\frac{\partial}{\partial x_i}\left(\rho k u_i\right)=\frac{\partial}{\partial x_j}\left[\alpha_k\left(u+u_t\right)\frac{\partial k}{\partial x_j}\right]+G_k-\rho\varepsilon \tag{4}$$

$$\frac{\partial}{\partial t}\left(\rho\varepsilon\right)+\frac{\partial}{\partial x_i}\left(\rho\varepsilon u_i\right)=\frac{\partial}{\partial x_j}\left[\alpha_\varepsilon\left(u+u_t\right)\frac{\partial\varepsilon}{\partial x_j}\right]+C_{1\varepsilon}^{*}G_k\frac{\varepsilon}{k}-C_{2\varepsilon}\rho\frac{\varepsilon^2}{k} \tag{5}$$

There,

$$\mu_t=\rho C_\mu\frac{k^2}{\varepsilon}\qquad C_{1\varepsilon}^{*}=C_{1\varepsilon}-\frac{\eta\left(1-\frac{\eta}{\eta_0}\right)}{1+\beta\eta^3}$$
$$\eta=\left(2E_{ij}\cdot E_{ij}\right)^{\frac{1}{2}}\frac{k}{\varepsilon}\qquad E_{ij}=\frac{1}{2}\left(\frac{\partial u_i}{\partial x_j}+\frac{\partial u_j}{\partial x_i}\right) \tag{6}$$

Here, G_k is the turbulent flow energy; it is the main difference between the RNG model and the standard model. C_μ=0.0845, η_0=4.38, β=0.012, $\alpha_k=\alpha_\varepsilon\approx$1.393, are the inverse Prandtl constant in turbulent and dissipative equations, respectively.

2.3 Numerical calculation method and initial condition

In this paper, Reynolds averaged numerical simulation (RANS) and Realizable k-ε turbulence model is adopted based on the finite volume method. The fluid pressure-velocity coupling is adopted in the solving process, and the two-order upwind difference scheme is used to solve the general governing equations based on the SIMPLE algorithm. The high temperature primary temperature of the wall covering is a local value, but in some cases, it is assumed to be a constant, or assumed to be equal to the total temperature of the gas. Coolant temperature is generally set to the temperature at which coolant enters the main outlet point, but for the compression stream, coolant temperature is more suitable set to covering temperature, or overall temperature. The adiabatic wall temperature is the temperature of the local mixed fluid, which flows from the gas to the wall, or from the wall to the gas. The parameters of film cooling structure include blowing ratio, momentum flow ratio, velocity ratio, density ratio, temperature ratio, surface curve, edge thickness, freestream Mach number and free stream turbulence intensity. These parameters and their interactions determine the initial film cooling efficiency at the incident point, and the attenuation of the cooling efficiency of the downstream gas film.

Initial condition parameters are approximated by a set of actual data provided by a Turbine Research Institute. The working environment pressure is P=2.5×10^6 Pa. Mainstream, the velocity and temperature were respectively set to U_∞=300 m·s^{-1} and T_∞=1900 K; Jet flow cooling air temperature T_c=900 K. The jet velocity is given according to different blowing ratios.

3. Analysis and Discussion of Results

3.1 The basic indicators for evaluating cooling effectiveness

The following 3 indexes are used to evaluate the cooling effect of gas film on blade metal.

(1) Blowing ratio M

The blow ratio is defined as [20]:

$$M=\frac{\rho_c U_c}{\rho_\infty U_\infty} \tag{7}$$

where ρ_c and ρ_∞ are the density of jet and mainstream; U_c and U_∞ are jet flow and mainstream flow velocity, respectively. The blowing ratio is essentially the ratio of

the mass flow rate of the jet to that of the mainstream. The larger the blowing ratio, the larger the mass flow rate of the jet.

(2) Film cooling efficiency η

The film cooling efficiency is defined as:

$$\eta=\frac{T_\infty - T_{aw}}{T_\infty - T_c} \tag{8}$$

where T_∞, T_{aw} and T_c are the mainstream gas temperature, adiabatic wall temperature and jet flow temperature, respectively. η is an important parameter for measuring film cooling characteristics. The higher the η value, the closer the temperature of the two streams to the temperature near the wall.

(3) Effective film coverage ratio A_f

In film cooling, gas film is generally required to be uniform and widely distributed on the cooling wall. Therefore, the effective film coverage area becomes an important factor to evaluate the film cooling quality. The effective film coverage ratio is defined as A_f [21].

$$A_f = \frac{a_f}{a_h} \tag{9}$$

where a_f and a_h are the effective gas film coverage area and cross section area of refrigerant conveying channel, m^2; In view of the thermal properties and inflow temperature of turbine blades provided by a research institute [21], it is considered that the effective coverage of gas film is the area of $\eta \geq 0.3$, that is the area of surface temperature $T_{aw} \leq 1600$ K. By calculating the effective film coverage ratio of A_f, the film cooling performance can be better estimated.

3.2 Cooling characteristics of film cooling hole with micro-groove structure

Firstly, the characteristics of velocity field, temperature field and cooling efficiency during film hole cooling with micro-groove structure are analyzed when M=1.0. Fig. 2 shows the velocity distribution of the central plane in the micro-groove of the film hole with micro-groove structure. Fig. 2(a) shows that eddy currents are generated at the interval of the jet holes at the initial stage in the microchannel. After a certain distance, the air flow develops and diffuses in the groove, which can fill the whole groove. This can also be seen from the velocity curve in Fig. 2(b). The velocity varies obviously in the affected and non-affected regions of the jet flow in the micro-groove, and fluctuates sharply when the airflow just enters the micro-groove from the micro holes (x/D=5). With the full development of air flow in the micro-groove, the gap between the two becomes smaller and smaller (x/D=7). It is also the reason that the film cooling surface has a larger coverage area at the direction vertical to the flow.

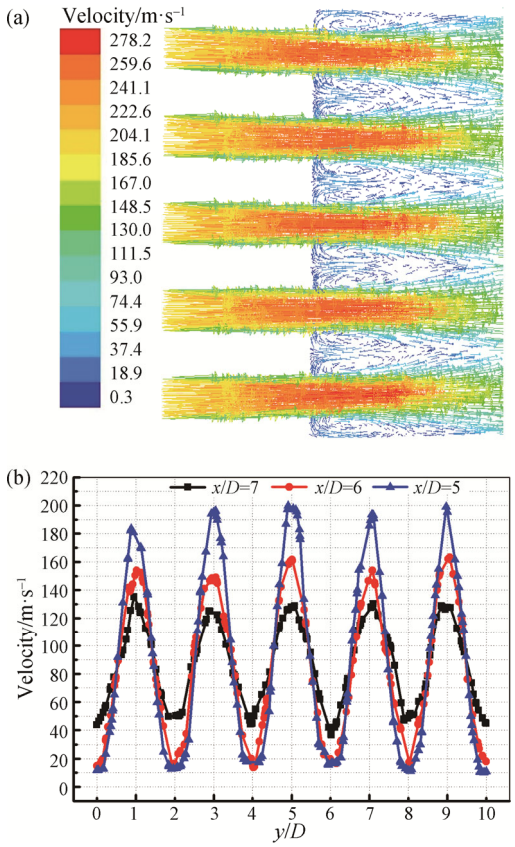

Fig. 2 Velocity at central plane for micro-groove: (a) Velocity vectors and (b) Velocity curves vertical to the flow direction at different entrance distances

Fig. 3 shows the temperature distribution on the film cooling surface. From the temperature distribution cloud chart, it can be seen that a fully covered film can be formed on the cooling surface. The temperature in the jet region of the film hole is lower and the temperature in the interval region is higher. However, with the full development of the flow field, the gap between the two is gradually reduced. It can also be seen from the figure that the maximum temperature is about 1600 K at x/D=30 from the outlet.

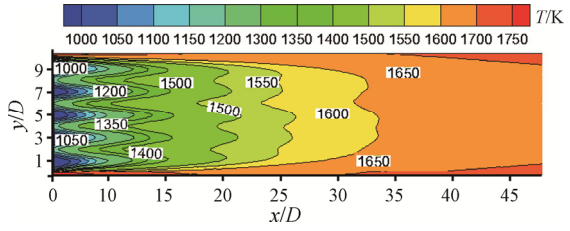

Fig. 3 Temperature distribution on film cooling surface

Fig. 4 shows the cooling efficiency variation curve of film cooling surface at different positions. Fig. 4(a) shows the cooling efficiency variation curve vertical to the flow direction at different distances from outlet.

Fig. 4(b) shows the cooling efficiency variation curve along the flow direction. Line y=0 denotes the central position of the jet hole and line y=0.5 denotes the interval position of two jet holes. In Fig. 4(a), it can be seen that near the outlet of the micro-groove, the cooling efficiency of the cooling surface is higher, and the size fluctuation is obvious. With the distance increasing, the cooling efficiency becomes lower and the size is close. The cooling efficiency is about 0.4 at x/D=15. In Fig. 4(b), it can be seen that at the initial stage, the cooling efficiency at Y=0 is higher than that at y=0.5, but the two approaches gradually along the flow direction. But even at the interval (y=0.5) between the two holes, the cooling efficiency is quite high. At x/D=30, the cooling efficiency is still effective ($\eta \geq 0.3$).

In addition, for the film holes of the micro-groove structure, the cooling efficiencies at different blowing ratios and different cooling air temperature were compared. Fig. 5 shows effect of blowing ratio on cooling efficiency at central of film cooling surface. Fig. 6 shows effect of jet flow temperature on cooling efficiency at central of film cooling surface. As can be seen from the figure, with the increase of blowing ratio, the surface cooling efficiency increases gradually, which indirectly illustrates the good film surface adherence of the micro-groove structure film hole. When M=0.5 the

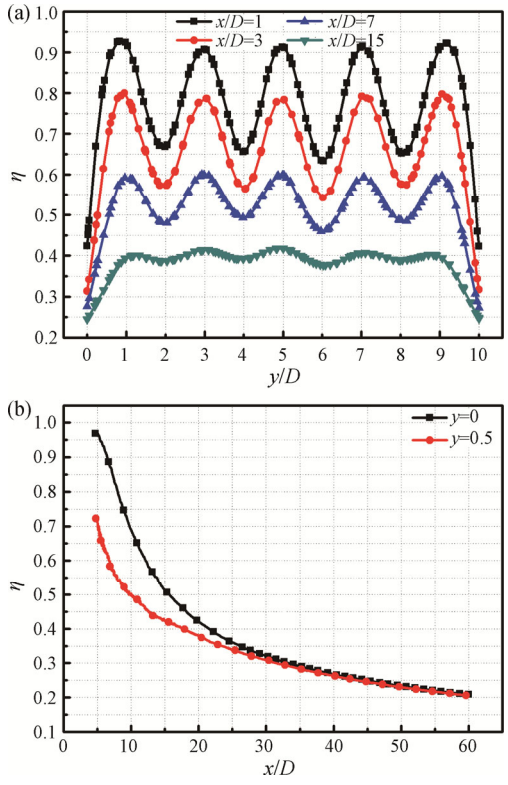

Fig. 4 Film cooling efficiency on film cooling surface (a) Vertical to the flow direction at different distances from outlet (b) Different positions at the flow direction

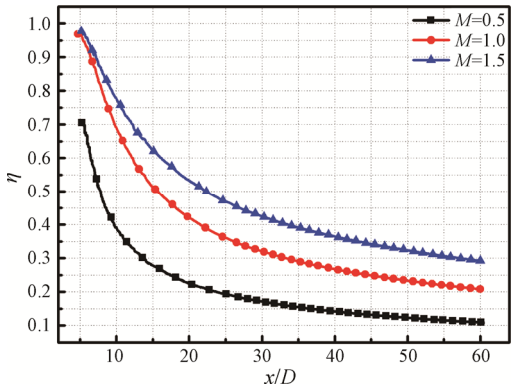

Fig. 5 Effect of blowing ratio on cooling efficiency at central of film cooling surface

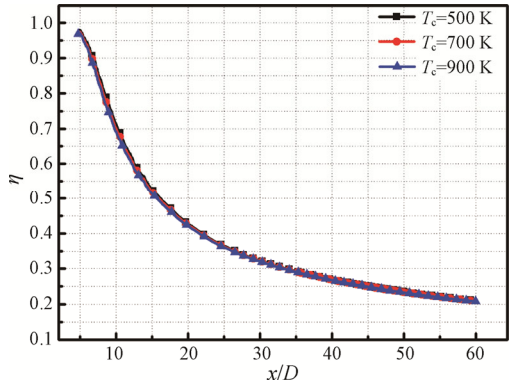

Fig. 6 Effect of jet flow temperature on cooling efficiency at central of film cooling surface

effective cooling distance on the surface is about x/D=13, and when M=1.0, this value is x/D=30. When M=1.5, the cooling efficiency of the whole length direction of the surface is effective. From Fig. 6, it can be seen that the influence of cooling air temperature on the cooling efficiency of film cooling surface is not obvious. This is because the amount of cooling gas flow is less than that of high-temperature gas flow. After heat exchange between high and low-temperature gases, the influence of cooling gas temperature is not significant.

Fig. 7 shows a comparison of film cooling efficiencies downstream of the film hole along the flow direction at M=1.0. In the figure, the cooling efficiency of cylindrical hole film studied by Lu et al. [6] is compared. In their research, the inclination angle of cylindrical hole is 30°, and the spacing of cylindrical hole is three times the diameter of hole, which are similar to the research in this paper, so it has certain comparability. As can be seen from the figure, there are some differences between the two cylindrical holes, which is due to the different velocity and temperature values of the cooling flow. But the cooling efficiency of the micro-groove structure hole proposed in this paper is obviously higher than that of the cylindrical hole.

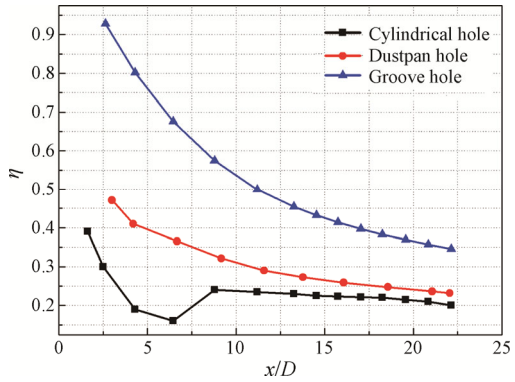

Fig. 7 The comparison of film cooling efficiencies downstream of the film hole along the flow direction at M=1.0

3.3 Comparison of cooling characteristics with traditional film hole

In view of the film cooling characteristics of the micro-groove structure, a comparison is made between the traditional cylindrical hole and the special-shaped hole of the dustpan. Fig. 8 shows (M=1.0) the temperature distribution on the cooling surface under film cooling with different film holes. From the temperature distribution cloud chart, it can be seen that the influence area of film on the cooling surface of cylindrical holes is small, and that in some areas where holes exist, the temperature affected by film is lower, while in the area between holes, the temperature is higher. The maximum temperature is over 1600 K at x/D=20 downstream of the hole. The influence area of film on cooling surface of special-shaped hole of dustpan is obviously higher than that of cylindrical hole. The maximum temperature can reach more than 1600 K only at x/D=35 downstream of the hole. But at the direction of width, the influence area of cylindrical hole and dustpan shaped hole is very limited, only limited to the width of hole. The microgroove structure has an effect on the whole surface, and the temperature in the long direction is also lower than the former.

Fig. 9 shows the cooling efficiency comparison of three kinds film cooling holes at the flow direction when M=1.0. Fig. 9(a) shows the cooling efficiency comparison at central of film cooling surface. The results show that the cooling efficiency near the outlet of the microchannel is higher and decreases gradually along the flow direction. Moreover, the cooling efficiency of the micro-groove structure hole and the special-shaped hole of dustpan is obviously higher than that of the cylindrical hole. The results also show that the film cooling efficiency of the special-shaped hole of dustpan and the cylindrical hole have been below 0.3 at x/D=25 downstream of the hole. However, when x/D=40, the cooling efficiency of the micro-groove structure hole is

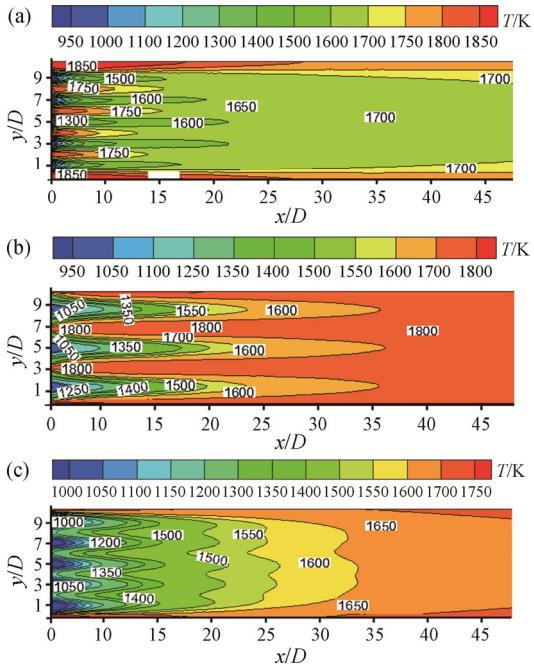

Fig. 8 Comparison of temperature distribution on film cooling surface of three kinds film cooling holes: cylindrical hole (a), dustpan hole (b), and groove hole (c) (M=1.0)

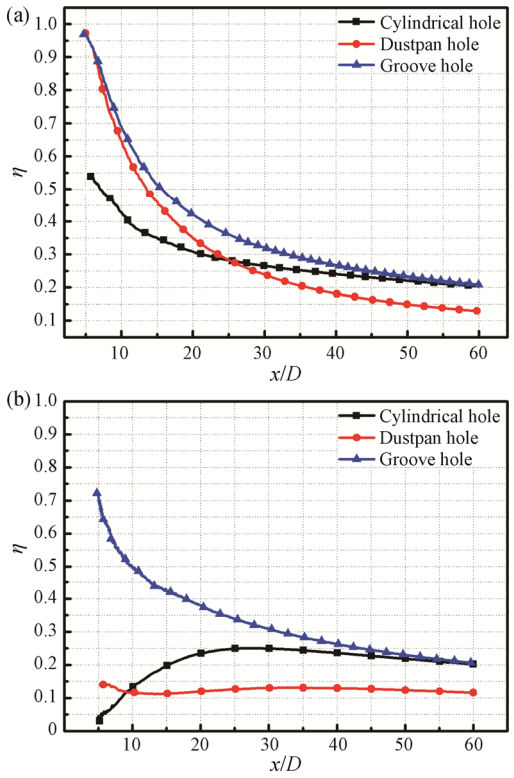

Fig. 9 Cooling efficiency comparison of three kinds film cooling holes at the flow direction: (a) at central of film cooling surface and (b) the middle of the interval (M=1.0)

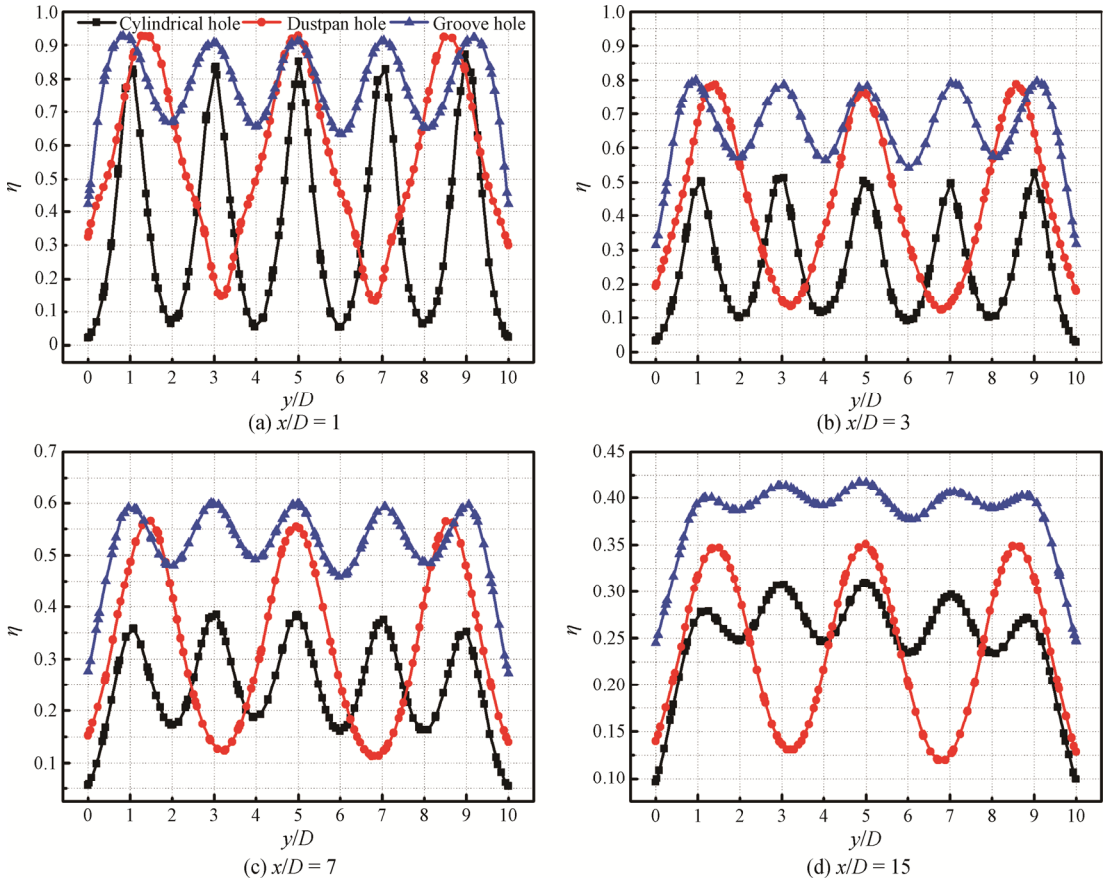

Fig. 10 Cooling efficiency comparison of three kinds film cooling holes at different positions vertical to the flow direction (M=1.0)

less than 0.3. Fig. 9(b) shows the cooling efficiency comparison at the middle of the interval. It can be seen the cooling efficiency of the special-shaped hole of dustpan and the cylindrical hole are less than 0.3, which is invalid. The cooling efficiency of the micro-groove structure hole is effective until x/D=35.

Fig. 10 shows the cooling efficiency comparison of three kinds film cooling holes at different positions vertical to the flow direction when M=1.0. It can be seen from the figure, the cooling efficiency at the outlet position varies greatly in the hole-affected zone and the non-affected zone. With the development of flow, the change of micro-groove structure hole decreases gradually. At x/D = 15, the cooling efficiency of the two regions is almost the same. Moreover, the cooling efficiency is greater than 0.3, which is considered to be effective. It can also be seen from the figure that the cooling efficiency of the special-shaped hole of dustpan and the cylindrical hole in the interval area is very poor.

Fig. 11 shows the effective film coverage ratio comparison of three kinds of film cooling holes at different blowing ratios. The effective film coverage ratio of three kinds film cooling holes when M=0.5 are closed between each structure. With the increase of blowing

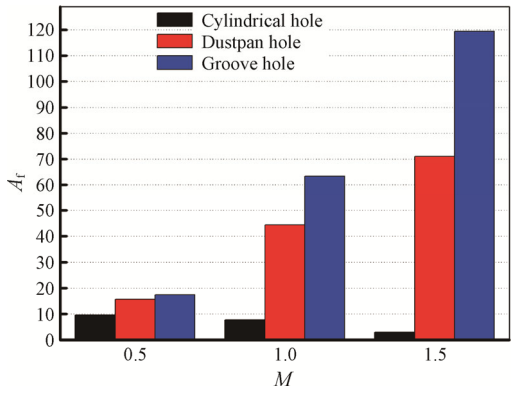

Fig. 11 Effective film coverage ratio comparison of three kinds film cooling holes at different blowing ratios

ratio, the effective coverage ratio of the micro-groove structure hole and the special-shaped hole of dustpan increases, while that of cylindrical holes decreases. This is because the adherence of the first two kinds of holes is better than the cylindrical holes. From Fig. 11, it can also be seen that the effective coverage ratio of the micro-groove holes is higher than the dustpan holes. For example, when M=1.5 the effective coverage ratio of micro-groove holes is 1.5 times the dustpan holes.

4. Conclusion

Film cooling technology is an effective method to improve engine cooling efficiency. In this paper, the cooling characteristics of film holes with micro-groove structure are studied by numerical simulation, and compared with traditional cylindrical holes and special-shaped holes of dustpan, the following conclusions can be drawn:

(1) Because the velocity at the outlet of the hole is affected by the vertical component of the inlet jet, the phenomenon of "jet" appears. The momentum component of the jet perpendicular to the mainstream penetrates the mainstream boundary layer, and the protective effect of cooling air on the wall becomes worse. Therefore, the cooling efficiency of cylindrical holes is the worst. With the increase of the cross-section area of the dustpan outlet, the airflow decelerates, and the ability of the jet to penetrate the mainstream decreases, so the coverage is better than that of the cylindrical hole. Because of the effect of transverse groove, cooling air first flows out of the groove and diffuses in the groove, which reduces the momentum of the jet and further weakens the ability of the jet to penetrate the mainstream. Therefore, the film cooling effect is better than that of cylindrical hole and dustpan hole.

(2) The blowing ratio has a great influence on the cooling efficiency of film holes with different structures. The results show that with the increase of blowing ratio, the film cooling efficiency of cylindrical holes decreases significantly, and the effective film coverage ratio decreases. With the increase of blowing ratio, the momentum of jet increases. For dustpan holes and micro-groove holes, due to the good film attachment effect, the cooling efficiency increases. At the same time, the injection range perpendicular to the flow direction is larger, and the effective film coverage ratio becomes larger.

Acknowledgement

This work was supported by Key Deployment Projects of the Chinese Academy of Sciences (ZDRW-CN-2019-01), National Defense Basic Scientific Research Program (JCKY2016130B203), National Natural Science Foundation of China (U1609208).

References

[1] Goldstein R.J., Film cooling, advances in heat transfer. Academic Press, Salt Lake City, UT, USA, 1971, 7: 321–379.

[2] Goldstein R.J., Eckert E.R.G., Burggraf F., Effects of hole-geometry and density on three-dimensional film cooling. International Journal of Heat & Mass Transfer, 1974, 17: 595–607.

[3] Kruse H., Effects of hole geometry, wall curvature and pressure gradient on film cooling downstream of a single row. In AGARD Heat Transfer and Cooling in Gas Turbines 13 p (SEE N86-29823 21-07), 1985.

[4] Haven B.A., Yamagata D.K., Kurosaka M., Yamawaki S., Maya T., Anti kidney pair of vortices in shaped holes and their influence on film cooling effectiveness. Proceedings of the ASME Turbo Expo 1997, Paper 97-GT-45.

[5] Bunker R.S., A review of turbine shaped film cooling technology. Journal of Heat Transfer, 2005, 127: 441–453.

[6] Lu Y., Dhungel A., Ekkad S.V., Bunker R.S., Effect of trench width and depth on film cooling from cylindrical holes embedded in trenches. ASME Journal Turbomach, 2009, 131: 011003.

[7] Lee K.D., Kim K.Y., Optimization of a cylindrical film cooling hole using surrogate modeling. Numerical Heat Transfer Part A, 2009, 55 (4): 362–380.

[8] Kim J.H., Kim K.Y., Film-cooling performance of converged-inlet hole shapes. International Journal of Thermal Science, 2018, 124: 196–211.

[9] Davidson F.T., KistenMacher D.A., Bogard D.G., Film cooling with a thermal barrier coating: round holes craters, and trenches. ASME Journal Turbomachinery, 2014, 136: 041007.

[10] Zhang Z.J., Zhu X., Huang Y., Wang C.H., Investigation on film cooling performance from a row of round-to-slot holes on flat plate. International Journal of Thermal Science, 2017, 118: 207–225.

[11] Zhang B.L., Zhu H.R, Liu C.L, Yao C.Y., Fu Z.Y., Experimental and numerical research on heat transfer and flow characteristics in two-turn ribbed serpentine channel with lateral outflow. Experimental Thermal and Fluid Science, 2019, 104: 116–128.

[12] Karsten K., Anas E., Dieter B., Takao S., Ryozo T., Masahide K., The nekomimi cooling technology: cooling holes with ears for high-efficient film cooling. Proceedings of ASME Turbo Expo 2011, Vancouver, Canada, Paper GT2011-45524.

[13] Marc J.E., Jubran B.A., A numerical study on improving large angle film cooling performance through the use of sister holes. Numerical Heat Transfer, Part A, 2009, 55: 634–653.

[14] Liu Z., Yang X., Feng Z.P., Study on heat transfer and cooling in gas turbine blade: Film cooling. Thermal Turbine, 2014, 43: 1–9.

[15] Li S.H., Song D.H., Liu J.H., et al., Numerical simulations of flat plate film cooling using respectively different shaped jet holes. Proceedings of the Chinese Society for Electrical Engineering, 2006, 26: 112–116.

[16] Zhang D.H., Ren B., Liu S., Discuss on evaluation of film cooling uniformity. Turbine Technology, 2013, 55:

171–174.

[17] Zhou J.F., Wang X.J., Li J., Li Y.D., Effects of film cooling hole locations on flow and heat transfer characteristics of impingement/effusion cooling at turbine blade leading edge. International Journal of Heat & Mass Transfer, 2018, 126: 192–205.

[18] Zhu X.D., Zhang J.Z., Tan X.M., Numerical assessment of round-to-slot film cooling performances on a turbine blade under engine representative conditions. International Communications in Heat and Mass Transfer, 2019, 100: 98–110.

[19] Ye L., Liu C.L., Liu H.Y., Zhu H.R., Lu J.X., Experimental and numerical study on the effects of rib orientation angle on film cooling performance of compound angle holes. International Journal of Heat & Mass Transfer, 2018, 126: 1099–1112.

[20] Tang X.Z., Li L.P., Huang Z.J., et al., Influence of hole spacing on the film cooling effectiveness of a gas turbine moving blade. Journal of Chinese Society of Power Engineering, 2018, 38: 105–113.

[21] Lubman D.M. Lasers and mass spectrometry. Oxford: Oxford University Press, 1990.